Electronic Supplementary Material (ESI) for Dalton Transactions.

Supporting Information for

Photo-Induced Cytotoxicity and Anti-Metastatic Activity of Ruthenium(II)-Polypyridyl Complexes Functionalized with Tyrosine or Tryptophan

Vadde Ramu,[a] Sunil Aute[a], Nandaraj Taye,[b] Rweetuparna Guha,[a] Devraj Mogare,[b] Apoorva Parulekar,[b] Jim A Thomas,*[c] Samit Chattopadhyay*[b], and Amitava Das*[a]

[a]Organic Chemistry Division, CSIR-National Chemical Laboratory, Pune, 411008, India;

[b]Chromatin and Disease Biology Laboratory, National Center for Cell Science, Pune, 411007, India;

[c]Department of Chemistry, University of Sheffield, Sheffield, UK. E-mail: james.thomas@sheffield.ac.uk;

[d]Indian Institute of Chemical Biology, Kolkata: 700 032, West Bengal, India; E-mail: samit@iicb.res.in

[e]CSIR-Central Salt and marine Chemicals Research Institute, Bhavnagar, 364002, Gujarat, India E-mail: a.das@csmcri.res.in

Table of contents **Page No**

UV-Visible and fluorescence titration with CT-DNA

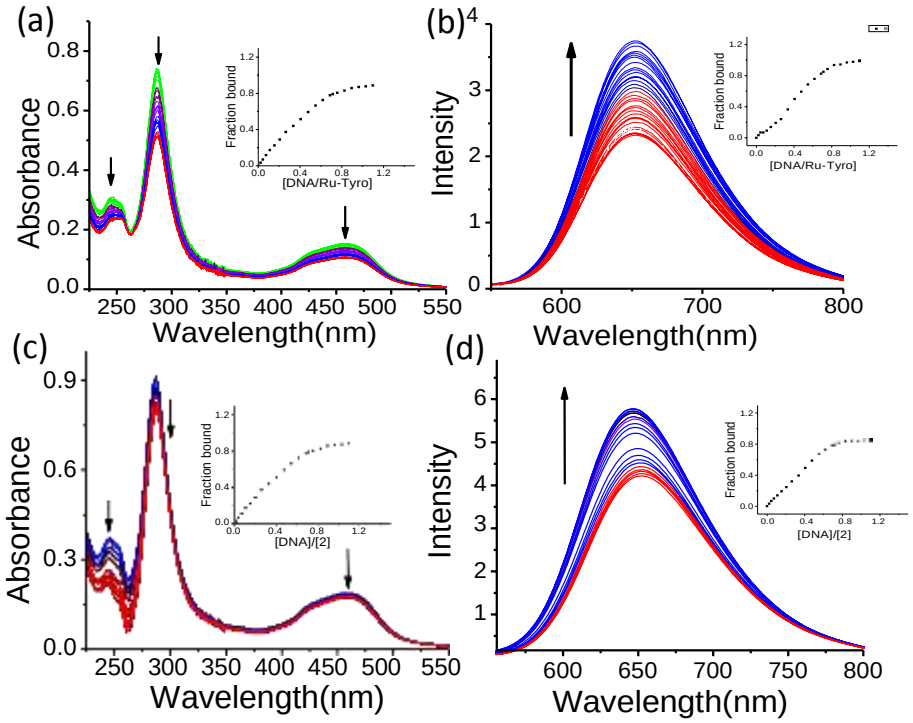

Figure S1. UV-Visible and fluorescence spectral changes for **1**(a, b) and **2**(c, d) by the addition of CT-DNA in Tris-HCl buffer pH = 7.4 at 25° C.

Viscosity measurements

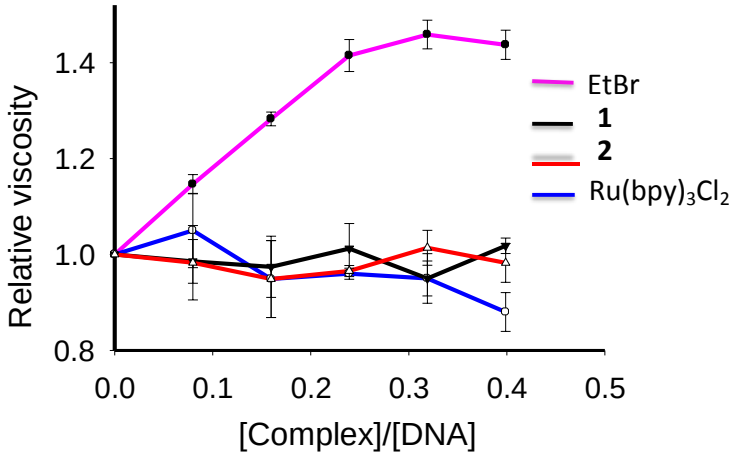

Figure S2. Viscosity changes of CT-DNA by the addition **1**, **2,** $Ru(bpy)_3Cl_2$ and ethediumbromide in Tris-HCl buffer pH = 7.4 at 25 ± ° C.

Singlet oxygen phosphorescence at 1275 nm

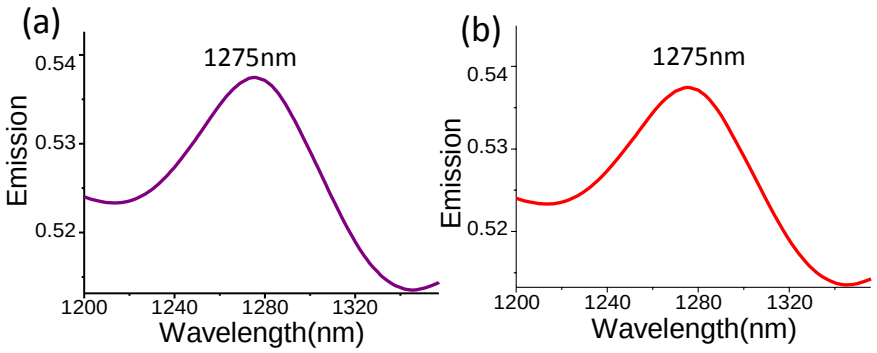

Figure S3. The $^1O_2$ fluorescence at 1275 nm was recorded in pure aqueous solution by the excitation of complex **1** and **2** at 455 nm.

Evaluation of $^1O_2$ production ability by 1 and 2

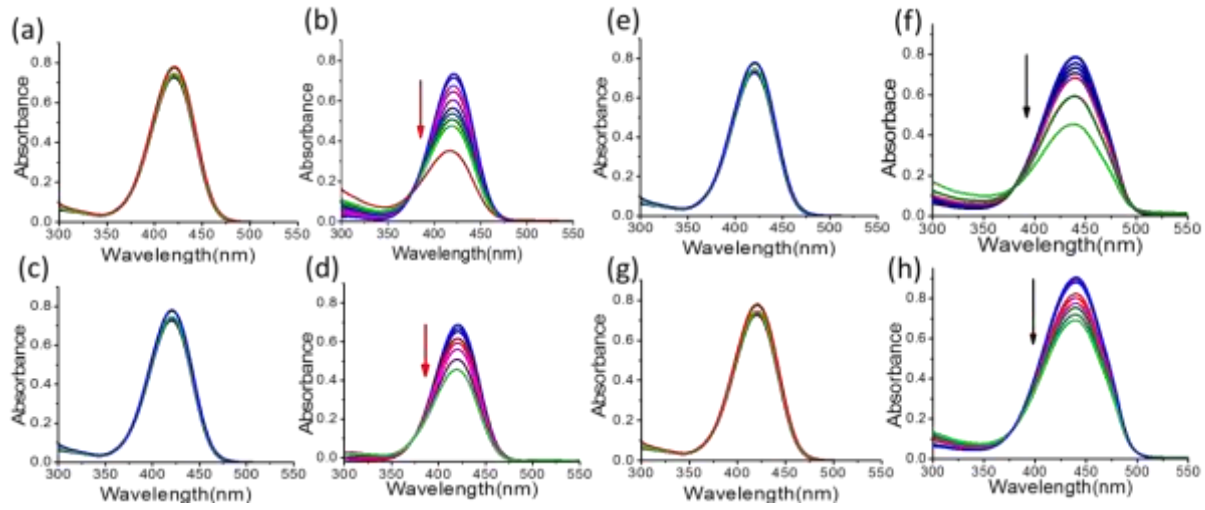

Figure S4. The detection of singlet oxygen in acetonitrile (a, b, e, f for **1**; and c, d, g, h for **2**) by indirect method; the photo-irradiation of **1** (b, f) and **2** (d, h) quenching absorbance of RNO in the presence of imidazole due to the generation of $^1O_2$. Dark treatment does not result any change in absorbance.

Photo-induced cytotoxicity of 1 and 2 in 3D tumor cell lines

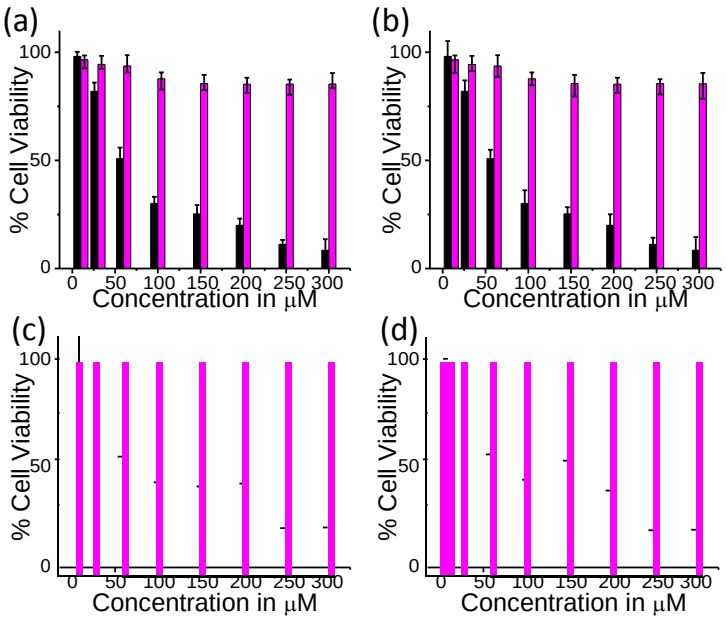

Figure S5. Photo-induced cytotoxicity of 1 (a, c) and 2 (c, d) in 3D tumors of A549 cells (top) and Hct116 (bottom) after photo-irradiation for 4 h (green bars), and in dark for 4 h (red bars).

Table S1. IC_{50} values for the complexes **1** and **2** incubated with A549 and Hct116 2D, 3D tumor cells in the dark and upon photo-irradiation.

	1						**2**					
	Dark		Light		PI		Dark		Light		PI	
Cells	2D	3D	2D	3D	2D	3D	2D	3D	2D	3D	2D	3D
A549	>300	>300	28.1±0.2	58.2±0.2	>10	>5	>300	>300	25.3±0.2	62.8±0.5	>10	>5
Hct116	>300	>300	30.1±0.4	65.4±0.1	>9	>4.5	>300	>300	30.0±0.2	59.1±0.3	>10	>5

MTT assay in the presence of ROS scavengers

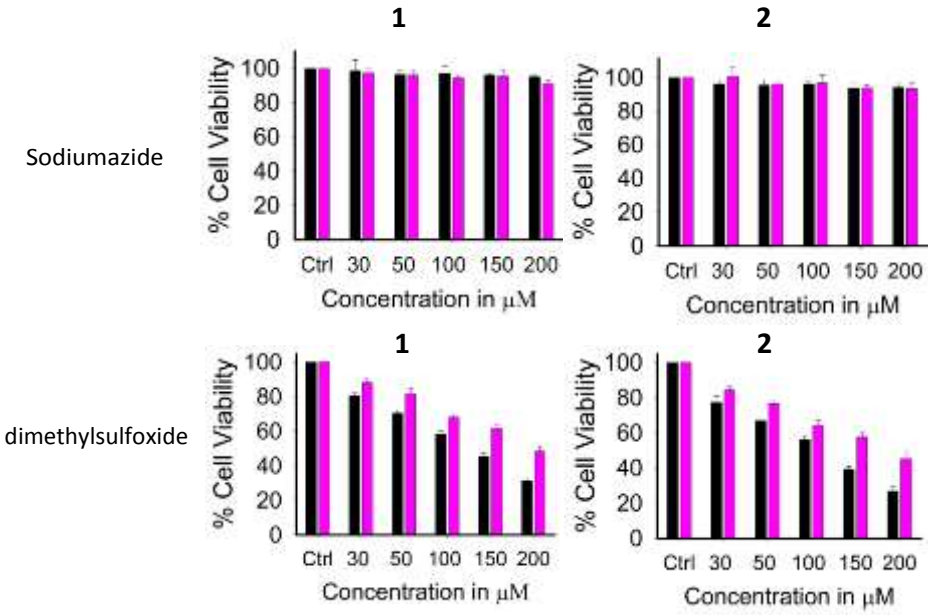

Figure S6. MTT assay results for the A549 cells incubated in the presence of ROS scavengers under photo irradiation conditions.

Percentage of DNA damage in cells: comet assay

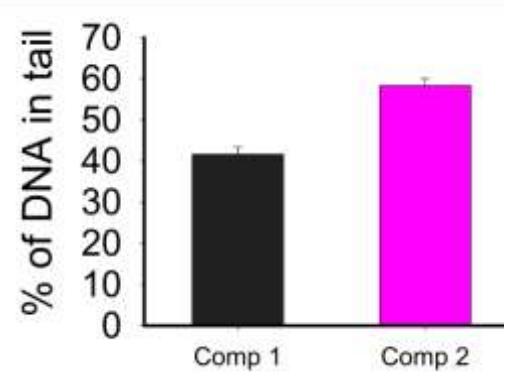

Figure S7. Percentage of DNA damage in at cellular level via comet assay measured using imageJ software.

Table S2. The cellular uptake quantification of **1** and **2** using MP-AES.

Complex	Log P Using shake-flask method	Ru accumulation ppm/ $1x10^6$ cells by MP-AES	
		Light	Dark
1	-1.31 ± 0.02	0.80ppm	0.18ppm
2	-1.72± 0.05	0.50ppm	0.11ppm

Characterization of complex 1 and 2[1]

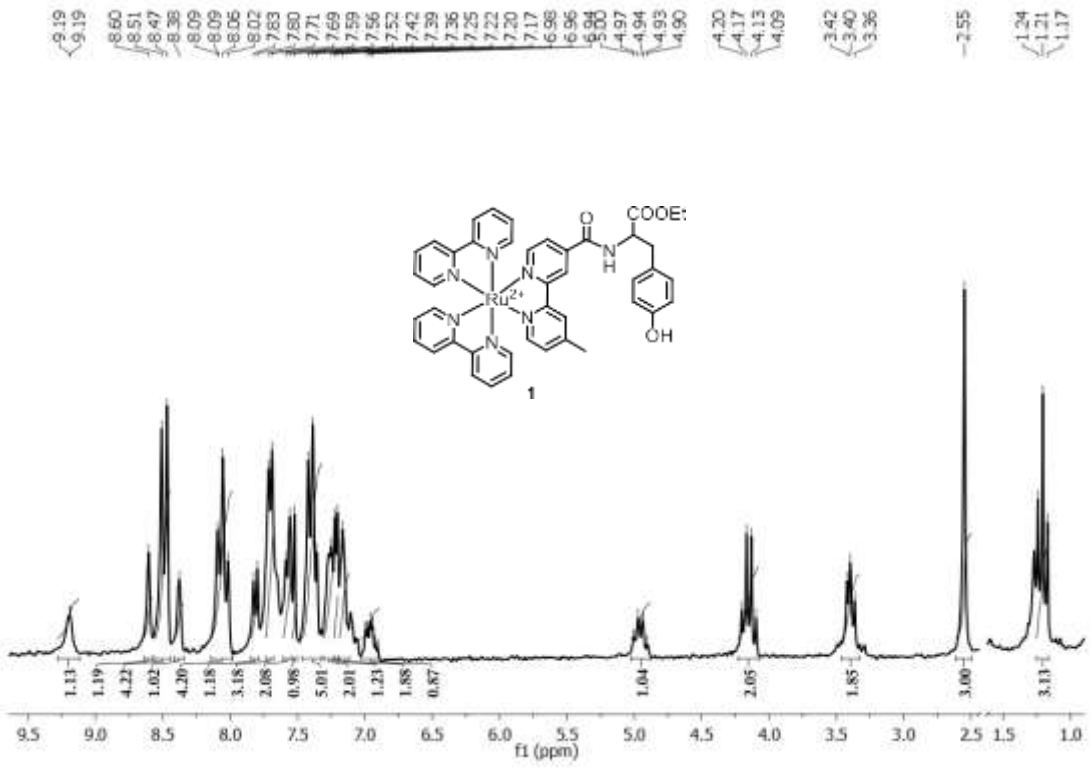

Figure S8. ^{1}H NMR spectra for complex **1** recorded in acetonitrile-d_3.

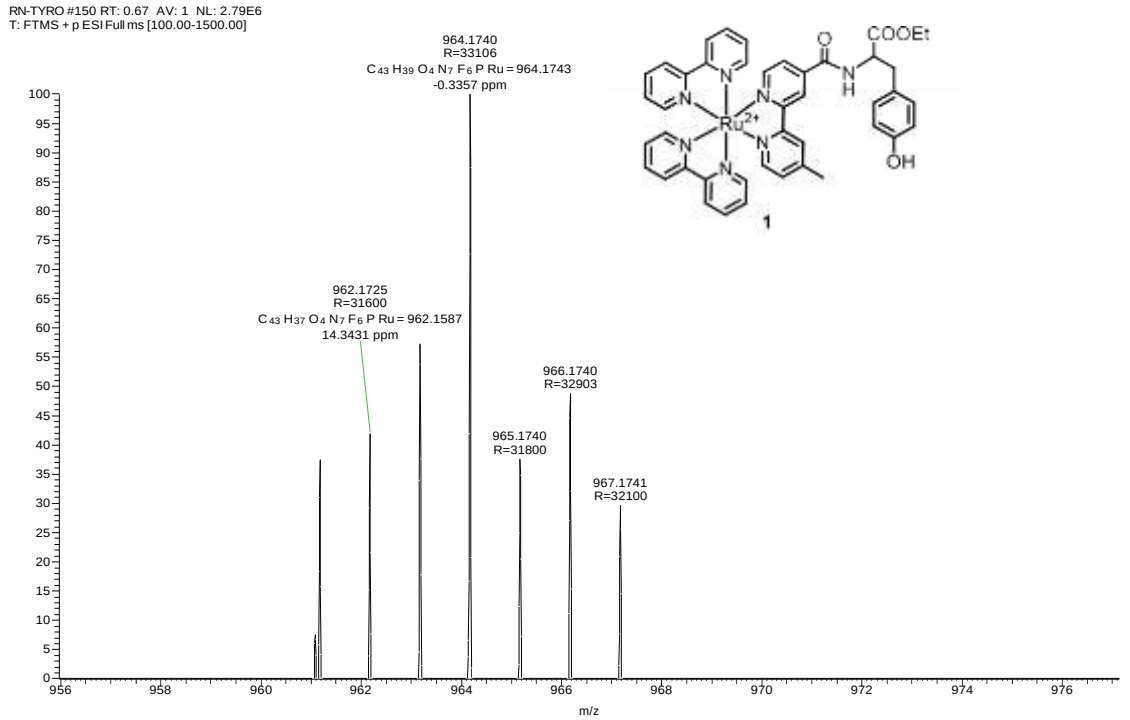

Figure

Figure S9. HRMS spectra for complex **1** recorded in acetonitrile.

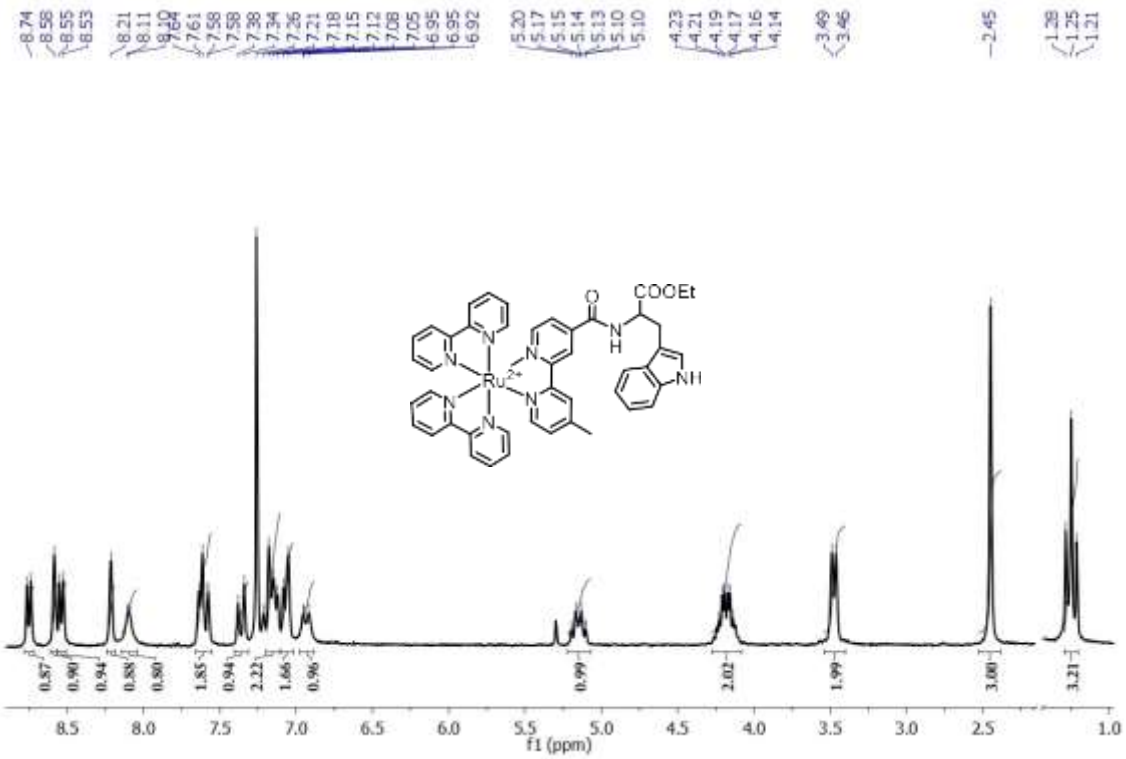

Figure S10. ^{1}H NMR spectra for complex **2** recorded in acetonitrile-d_3.

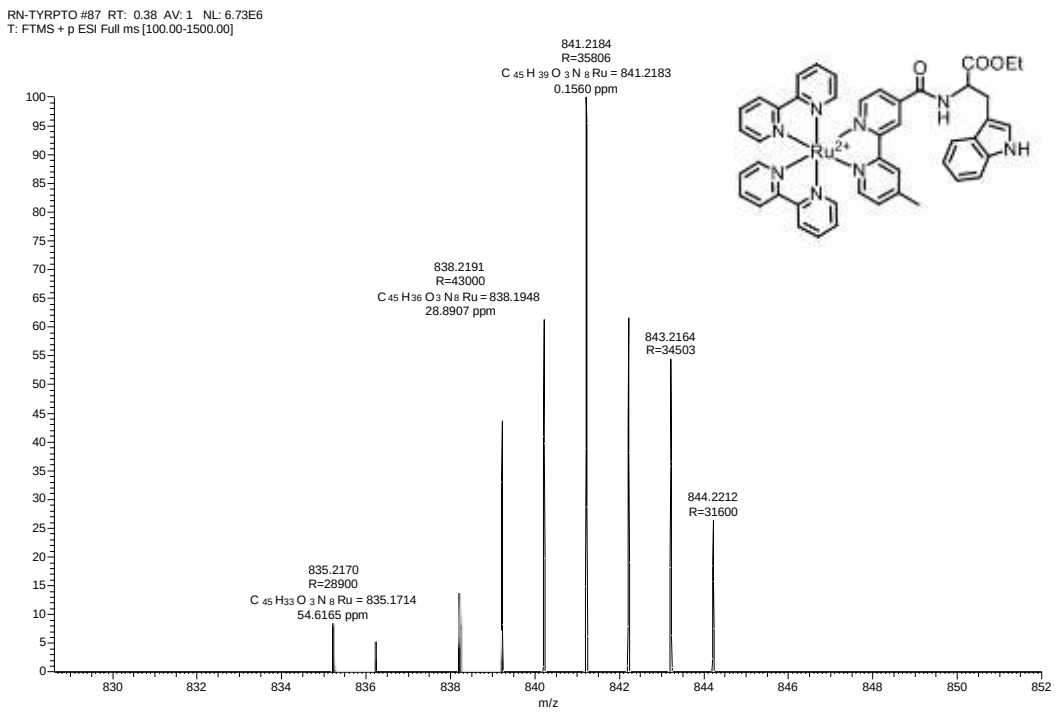

Figure S11. HRMS spectra for complex **2** recorded in acetonitrile.

Reference

(1) Sjödin, M.; Styring, S.; Wolpher, H.; Xu, Y.; Sun, L.; Hammarström, L. *J. Am. Chem. Soc.* **2005**, *127* (5), 3855–3863.